Bauhaus-Universität Weimar
20.-22. September 2022
BauSIM2022 in Weimar
ibpsa

ACOUSTIC TRAVEL-TIME TOMOGRAPHY: HIGHER LOCAL THERMAL COMFORT IN WORKPLACES OF THE FUTURE

Najmeh Sadat Dokhanchi [1], Jörg Arnold [1], Albert Vogel [1], Conrad Völker [1]
[1] *Department of Building Physics, Bauhaus-University Weimar, Deutschland,*
E-Mail: najmeh.sadat.dokhanchi@uni-weimar.de

Abstract

To assess the thermal comfort in the indoor spaces such as office rooms, generally thermal sensors are mounted in the workplaces. The main drawback of this conventional method is recording data at certain locations instead of distribution of the target parameter in the entire room including the occupant zone. To address this gap, the application of **A**coustic travel-time **TOM**ography (ATOM) is proposed which is based on the first order dependency of sound velocity on the air temperature. This study reports research on development of the ATOM measuring system at the Bauhaus-University Weimar to measure the indoor air temperature distribution. The measurement results reveal the applicability of the ATOM-measuring system for high-resolution monitoring of air temperature distribution in the workplaces of the future.

Introduction

For evaluation of a thermally comfortable indoor environment, monitoring the air temperature and air flow are of importance. The conventional thermal and flow sensors such as thermostats/thermistors and anemometers are used for monitoring these parameters which are normally mounted in the workplaces. However, these conventional sensors provide the local point measurements meaning that the recording data is limited to the installation location. Hence, for measuring the distribution of the air temperature and flow velocity, multiple thermal and flow sensors should be installed in the area under investigation. This requires high effort in both installation and expense. Moreover, mounting multiple sensors directly in the measurement environment (e.g., airflow sensors) is problematic due to their interference effect on the measured parameters itself. **A**coustic travel-time **TOM**ography (ATOM) offers an alternative to these traditional sensor networks based on measuring the transmission sound velocity signals. It allows for not only many more data points to be generated per sensor but also non-contact and non-destructive measurements. ATOM relies on the principle that the sound velocity of a medium is a function of medium's physical properties. In tomography of the indoor climate which is one of the most recent applications of ATOM, the medium properties of interest are the air temperature and air flow velocity fields. The other applications of ATOM vary ranging from seismology, oceanography and medical imaging to industry and meteorological studies. For instance, in industrial applications, this technique is vital for measuring gas temperatures in boilers, furnaces, and flue combustion chambers where the sensors cannot be placed directly in the measurement area (Srinivasan et al., 2013). For outdoor climate monitoring, meteorologists apply this technique to simultaneously measure the near-surface atmospheric temperature and wind velocity fields (Ziemann et al., 2002). Under the free field, the travel times of the direct sound paths between the transmitters and receivers with known distances will be considered for sound velocities calculation.

The transfer of ATOM in the indoor climate opened up a possibility to combine the room acoustics with the tomography techniques. Unlike the free field, when a sound wave is transmitted in a room, it is reflected numerous times at the room boundaries, thus not only the direct sound path but also a series of delay reflections reaching the receiver (Vorländer, 2008). Taking advantage of the room acoustics, it is possible for the reflections within an interval of so-called “early reflections” to be involved in the travel time analysis. The response of the room (RIR) to the transmitted excitation signal delivers perfectly the travel times of the direct sound path, early reflections and the late reverberation. In parallel to the measured travel-times from RIR, the simulated travel-times can be derived by applying the image source model (ISM). When the travel-times along the desired reflections are known, the sound velocities can be determined by dividing the length of the sound paths from simulation model to the measured travel times. Accordingly, the measured sound velocities can be converted into spatial air temperature distribution by applying a proper tomography algorithm. Prior to the tomography application, the volume of the room is divided into several voxels whilst the distribution of the reciprocal value of the sound velocity i.e. slowness is assumed to be constant within each voxel. The approach of utilizing high-energy early reflections in addition to the travel time of the direct sound was proposed initially by Bleisteiner et al. (Bleisteiner et al., 2016).

They developed a measuring system in which the spatially differentiated room air temperature with only one loudspeaker and one microphone was determined with the intention of using as little hardware as possible. The further development of ATOM for indoor climate measurements was performed as part of a project at the Chair of Building Physics at the Bauhaus-Universität Weimar. ATOM was used to measure the three-dimensional air temperature distribution in a rectangular room considering the approach of utilizing high-energy early reflections. The results of the extensive measurements in a climate chamber lab using one omnidirectional loudspeaker and one omnidirectional receiver are published in (Dokhanchi et al., 2019; Dokhanchi et al., 2020a, 2020b). In the present study, a newly developed measurement setup is presented, consisting of an array of two directional loudspeakers and one omnidirectional receiver. The measurement setup offers several advantages, such as improving the estimation of travel-times due to the directivity of the sound sources, providing higher number of well-detected early reflections for the tomography reconstruction, as well as a better space utilization. This paper first reviews the parameters that are involved in the resolution enhancement of the designed measuring system. Second, practical approaches leading to minimize the total amount of system's uncertainties are discussed. Following that, the results of empirical measurements for the analysis of the described methods are outlined. Finally, the accuracy of the measuring system is quantified for the designed measuring setup.

Problem Formulation

Identifying the sources of error

The main input parameters for the tomography algorithm for reconstructing the air temperature distribution are the travel-times of the signal to the receiver and the lengths of the sound paths between the transducers. One of the main parameters affecting the travel time estimation is the coordinates of the applied sound transducers in the test room. The coordinates of the transducers affect not only the length of the sound paths and thus the distribution of reflections in the RIR reflectogram, but also the distribution of the sound paths across the room. The sound velocities derived along the sound paths are very sensitive to the displacement errors that can be occurred during the positioning of the transducers. The sound velocities for each sound path can be calculated as follows:

$$l + \epsilon_l = c(\tau + \epsilon_\tau), \qquad c = \frac{l + \epsilon_l}{\tau + \epsilon_\tau} \qquad \text{[m/s]} \qquad (1)$$

Where c is the sound velocity, l is the length of the sound path, τ is the travel time and ϵ_l and ϵ_τ are the discrepancies for the length of the path and the travel time estimation, respectively. Accordingly, the sampling frequency of the measuring device specifies the smallest measurable sound velocity variation. Considering a sampling rate of 216 kHz, the time step of $\Delta\tau = 1/216000$ s for a sound velocity of $c = 343.421$ m/s at $\theta = 20$ °C allows a theoretical length resolution of ca. $l = 0.0016$ m. In other words, a deviation of the travel time ($\epsilon_\tau = 4.63 \cdot 10^{-6}$s) in the measured RIR corresponds to a distance shift of ca. $\epsilon_l = 0.0016$ m between the transducers. To reduce ϵ_l, it is therefore crucial to know the exact emitting point of the loudspeaker, which will be discussed in the next chapter.

Furthermore, the directivity of the sound sources is another criterion that should be considered when measuring the RIR. Loudspeakers emit a unique frequency dependent radiation pattern known as directivity depending on their physical construction and manufacturing material. The directivity of the loudspeaker determines the angle and relative level of sound that is radiated into a room thus significantly affecting the arrival time of the direct path and early reflections at the receiver position. In this regard, the room acoustic parameters for the description of the statistical sound field are commonly quantified using omnidirectional sound sources and receivers. For the reverberation time, which can be described for example by the energy decay of RIRs, the use of omnidirectional transducers is reasonable. For the ATOM technique, however, a more detailed analysis of the early reflections is required with respect to reflection detection. In this context, a suitable directional transducer can allow a substantial improvement of the SNR (signal-to-noise ratio) of the individual reflection paths.

Another parameter for improving the resolution concerns the number of sound travel-times that can be used as input data for the inverse algorithm. The quality of the reconstruction results of tomography algorithms can be significantly improved by a higher number of well-detected travel times, since the ratio of data to unknowns is increased (Fischer et al., 2012). Therefore, it is advantageous if several sound sources can be accommodated in a measurement setup. Moreover, with the aim of using the measuring system in the workplaces, the distribution of the transducers inside the measurement environment should not disturb the function of the room. Thus, it would be effective to design a measurement setup that can be reduced the practical limitations on the usage of the space.

Methodology

Design of the measurement set-up

A new measurement setup was developed with a focus on minimizing the described sources of error. It consists of an array of directional sound sources on the

perimeter of the floor while an omnidirectional receiver is placed at the middle of the room near the ceiling. Figure 1 shows an array layout inside the rectangular dimension (2.98 m × 2.99 m × 2.41 m) of the climate chamber lab. Placing an omnidirectional receiver at the middle of the room near the ceiling allows the sound paths to travel through all parts of the room to reach the receiver point. Thus, by using only one receiver, the coverage of the room with sound paths can be effectively ensured. Accordingly, utilizing directional sound sources allows to track early reflections longer in time since only a part of the reflections presents in the response, and there are fewer overlapping reflections. Additionally, distributing the transducers along the perimeter of the floor would eliminate any practical limitations on the usage of the space. As a result, any disruption of users' activities at workplaces caused by the placement of transducers can be minimized.

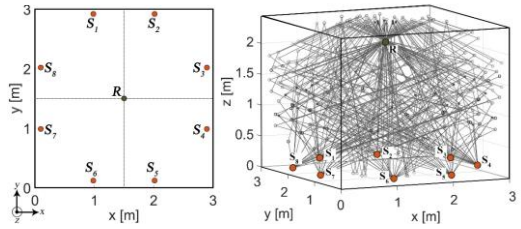

Figure 1: Suggested layout for an array of eight directional sources on the perimeter of floor and one omnidirectional receiver at the middle of room near the ceiling and the spatial distribution of sound paths

Furthermore, the design feature of the proposed array facilitates the addition of new sound sources up to a certain number to the set-up, thus a higher number of well-detected travel-times for tomography reconstruction can be achieved.

Distribution of early reflections in RIR

The distinguishability of travel-times plays an important role in travel-times detection; the more the desired travel-times are separated, the better they can be selected. As it is described, one of the key factors affecting the distribution of travel-times in the RIR reflectogram is the location of transducers inside the room. To find the optimal locations for placement of the transducers, the numerical method proposed in (Dokhanchi et al., 2020a) has been applied in which the implementation of the method was adjusted according to the boundary conditions of the new set-up. The transducers considered in the optimization method include one omni-directional receiver and one directional sound source with the practical beam spreading angle of $\theta = 120°$ at frequency range of 4000 Hz. To provide the total number of feasible locations for placement of the transducers, the searched areas are divided into 20 certain bins as it is shown by blue dots in Figure 2. In terms of the coverage of the room with sound paths, additional conditions have been applied to the proposed method provided in (Dokhanchi et al., 2020a). First, the number of walls hit by the sound paths was set to a maximum possible value. This boundary condition can ensure that the sound paths travel through different parts of the room as they can intersect with maximum discrete walls. Subsequently, another condition has been applied to the optimization method in which the number of simulated sound paths was set to be above an arbitrary value. As a result, those coordinates that produce the least number of early reflections given the angle of directivity of the sound source can be excluded from the calculation.

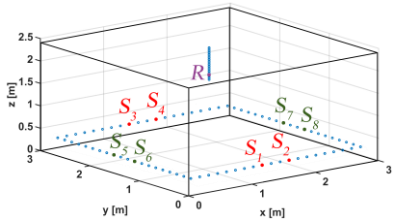

Figure 2: Optimal positions calculation- blue dots: the total feasible locations for placement of the transducers, red dots and green dots: the calculated optimal positions in x and y direction respectively, violet dot: the calculated receiver's position

Since the room is rectangular and the omnidirectional receiver is positioned in the middle, there are 4 optimal positions in the x-direction that have the same distribution of reflections in the RIR reflectogram. (S_1, S_2, S_3 and S_4 in Fig. 2). The reasons are the symmetry of the room geometry as well as the same position of the receiver for each loudspeaker-receiver combination. This principle is the same with the y-direction in which by mirroring the 2 calculated optimal positions derived from numerical method (S_5 and S_6), the total number of 4 optimal coordinates can be achieved in y-directions (green dots in Fig. 2). Figure 3 shows the simulated reflectogram derived from ISM method for one the source- receiver combinations placed at the calculated optimal positions. It is shown that the travel times up to third order image sources are perfectly separated and mapped in an appropriate distance from each other.

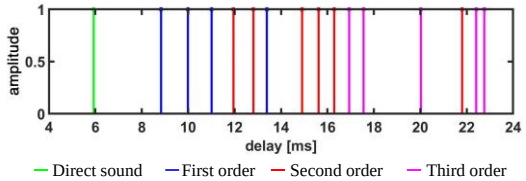

Figure 3: The simulated reflectogram for placement of transducers at optimal coordinates

Measuring the acoustic centre of the sound source

The accuracy with which the sound transducers can be positioned in the room has a significant influence on

the accuracy of the measured sound velocities. To minimize the uncertainties due to the positioning of the sound transducers, the exact emitting points of the loudspeaker, i.e. its acoustic centre (AC), was determined by measurement. The method used is based on the analysis of directional impulse responses described in (Franz et al., 2015). The acoustic centre was determined for different excitation signals with different frequency ranges. In this case, an MLS signal (order of n = 18, AC = +0.92 cm), a linear chirp (200 - 4000 Hz, AC = -0.83 cm) and a logarithmic chirp (200 -4000 Hz, AC = -0.92 cm) were used. A comprehensive comparison was made to determine the effect of the used excitation signal on the determined sound travel-times and thus room air temperatures in the climate chamber. For this travel time analysis, the differences between measured and simulated travel times for the individual sound paths were determined for each excitation signal. Subsequently, the variances for the travel time deviations were determined for 15 measurement repetitions. The linear chirp signal (200 - 4000 Hz) proved to be the optimum excitation signal for the given measurement conditions in the climate chamber, thus it was used for the further measurements.

Experiment

The developed set up was tested using only two directional sound sources placed at the two calculated optimal coordinates (S_6 and S_7 in Fig. 2). The reason is to keep the number of transducers as few as possible. Figure 4 shows the experimental set-up in the climate chamber.

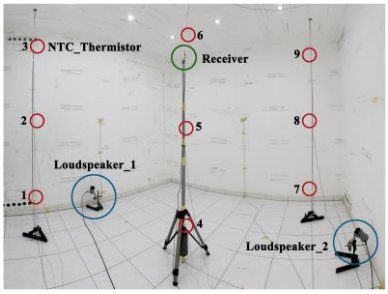

Figure 4: The experimental set-up in the climate chamber lab. The nine NTC sensors are located at the centre of 9 of 27 superimposed tomography voxels.

The measurement set-up was tested for both stationary and non-stationary conditions. Under the stationary condition, measurements were conducted for the four temperatures (21°C, 22°C, 23°C and 24°C). To reach a steady-state condition, the climate chamber was left overnight after each temperature change. For the temperature regulation, the interior surfaces of the chamber were set to the same temperature so that no natural convection could occur in the chamber. For the tomographic reconstruction, the volume of the chamber has been divided evenly into 27 voxels where the volume of each voxel is 0.99 m · 1.00 m · 0.80 m. To validate the ATOM reconstructed temperatures, nine NTC thermistors were placed at the centre of 9 of the 27 tomographic voxels (see Fig. 4). The tomographic algorithm for temperature field estimation is based on time-averaged RIR reflectograms for each loudspeaker-receiver combination, for which 10 measurement repetitions was set for averaging. Using the linear chirp signal for room excitation results in a measurement interval of 124 s, which includes the excitation times, the time of RIR averaging as well as the calculation time of the temperature field. A total of 15 sequential measurements of temperature were determined, resulting in a total measurement time of 31 minutes for each temperature (21 °C – 24 °C).

For the non-stationary condition, the experiment was conducted under a gradual air temperature drift from 22°C to 25°C in which the temperature of the entire surfaces of the chamber was increased simultaneously. As a result, a uniform transient condition can be achieved. The number of averaging of the RIR reflectograms for each loudspeaker-receiver combination was remained the same. Moreover, the total of 50 sequential temperature measurements were performed, resulting in 103 minutes total measurement time. For both stationary and non-stationary conditions, the measurement interval of the NTC thermistors was set to 1 s and synchronized with the ATOM measurement system. Subsequently, the ATOM temperatures of the nine voxels were compared with the time-averaged point temperatures of the NTC thermistors. In the measurement, two of the 2-inch broadband loudspeakers with the type of FRS 5 XTS by VISATON were used. The receiver was a standard 1/4-inch condenser microphone of type “AVM8 MI-17”. For contactless switching of speakers, the 8-way AC signal switch is designed which was connected to an amplifier output. For data acquisition, the measurement card `Data Translation “DT9847-2-2” was used, which is a dual channel dynamic signal analyser. The digitization rate of 216 kHz leads to a good time-resolution for the processing of signals. The software package used to analyse the data is MATLAB R2017b.

Measurement Results and Discussion

Figure 5 illustrates the comparison of the temperatures between the NTC thermistors and ATOM within the three superimposed voxels at the middle of the room under stationary conditions. The blue curves represent the recorded data from NTC-thermistors, and red curves depict the measured ATOM-temperatures. It is evident that the ATOM temperatures are in good agreement with the temperatures of corresponding NTC-thermistors. The recorded data from NTC thermistors (blue curves in Fig. 5) depicts a small vertical stratification of the air temperature at the location of the superimposed voxels. For the uniform temperature of 21 °C, the NTC thermistors illustrate a temperature gradient of about 0.06 °C between the

lower and upper voxels. This temperature gradient is about 0.11 °C at the temperature of 24 °C. However, ATOM barely exhibits this small vertical stratification in comparison to the NTC thermistors as shown by red curves in Figure 5. This can be explained through the inverse algorithm which stands for reconstructing the distribution of the temperature in each voxel. The tomography algorithm used in this study is the simultaneous iterative reconstruction technique (SIRT). Since the set of equations in the SIRT algorithm should be solved simultaneously, the reconstruction errors spread over all voxels. Hence, when the reconstruction error is low, it is more likely to observe uniform temperatures over the entire voxels rather than the minor temperature differences among the superimposed voxels. Moreover, it should be mentioned that unlike the NTC-thermistor that measures the temperature at its installation point, the ATOM-temperature represents the average temperatures in each voxel.

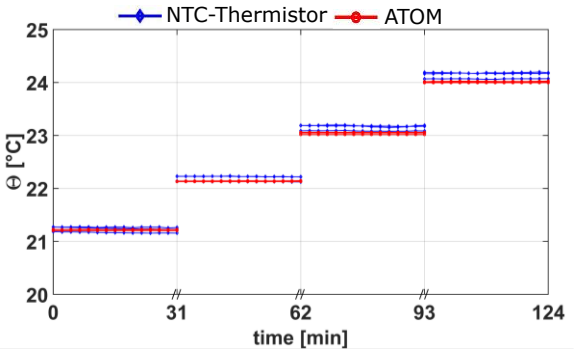

Figure 5: Comparison of temperatures between the NTC thermistors and ATOM within the three superimposed voxels in the middle of the room

In order to quantify the differences between the ATOM and NTC temperatures, the Root Mean Square Error (RMSE) was calculated for the selected 9 voxels. The box-plot in Figure 6 shows the calculated RMSE for each temperature.

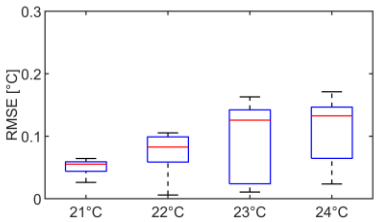

Figure 6: The RMSE between the ATOM temperatures and NTC thermistors over nine voxels

In this Figure, the black lines depict the maximum and minimum RMSE, red line is the median RMSE and blue lines represent the 80%/20% quantile RMSE. It can be seen that by increasing the temperature from 21 °C to 24 °C , the distribution of error is increased to some extent. Table 1 derived from Figure 6 shows the maximum (max), average (ave), median (med) and minimum (min) RMSE for every temperature. The average RMSE of 0.13°C was determined for temperature of 24 °C. This is primary due to inaccuracies between real and simulated room geometry, non-linearities of the transducers, but most importantly due to the discussed displacement errors that occur when placing the sources and receivers in the room.

Table 1: RMSE between ATOM and NTC thermistors over nine voxels - stationary conditions

T [°C]	MAX [°C]	AVE [°C]	MED [°C]	MIN [°C]
21	0.06	0.05	0.05	0.04
22	0.10	0.07	0.08	0.01
23	0.16	0.10	0.12	0.01
24	0.17	0.11	0.13	0.2

The distribution of the error in the plot-box in Figure 6 for the four temperatures can be associated with a three-dimensional representation of ATOM-temperature within 27 voxels shown in Figure 7. The color-bars are set to the temperature interval of 0.2 °C in which the variation of the ATOM-temperatures in each voxel can be observed (see Fig. 7). For the temperature of 21 °C, a uniform distribution of ATOM-temperatures over the entire voxels is well illustrated where the distribution of error is small (average RMSE of 0.05 °C outlined in table 1). However, as the temperature increases, a very small non-homogeneity of the temperature (less than 0.15 °C) due to the increased errors can be observed.

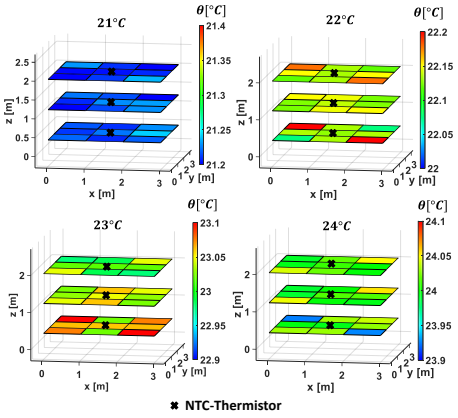

Figure 7: Relationship between the temperature variation in each voxel and the error rate for four temperatures. The colour-bars are set to the temperature interval of 0.2 °C

Figure 8 shows the results of the ATOM- temperatures for the non-stationary condition within the lower voxel in the middle of the room as an example. The ATOM-temperature (red curve) are compared with the corresponding NTC-thermistor (blue curve). It is evident that even under a transient condition, the ATOM measuring system can track the temperature

variations perfectly as the temperature are increased from 22 °C to 25 °C. As a result of simultaneously tempering six surfaces of the chamber, the temperature variations are uniform. This is well illustrated by Figure 9, which shows the distributions of ATOM-temperatures over 27 voxels for the elapsed times of 8 min and 50 min as an example.

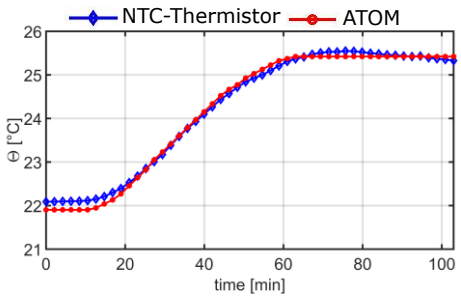

Figure 8: Non-stationary condition, comparison of temperatures between the NTC thermistors and ATOM within the lower voxel in the middle of the room

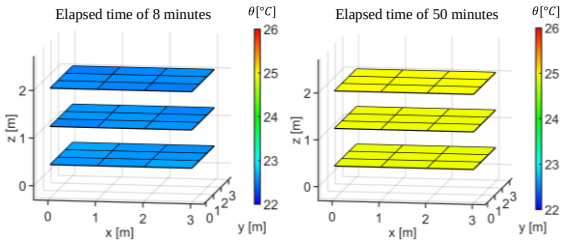

Figure 9: Non-stationary condition, 3D-representation of ATOM-temperature distribution

Table 2 shows the results of the calculated RMSE for the non-stationary condition. The average RMSE of 0.26 °C demonstrates an excellent performance of the ATOM measuring system even under transient condition.

Table 2: The RMSE between the ATOM temperatures and NTC thermistors over nine voxels for the non-stationary condition

CONDITIONS	MAX [°C]	AVE [°C]	MIN [°C]
NON-STATIONARY	0.39	0.26	0.12

Conclusions

This study proposed the applicability of using ATOM to monitor the air temperature distribution at the workplaces of the future with a high degree of resolution. Accordingly, a new measurement setup was developed which consists of an array of directional sound sources. The proposed set-up demonstrated several advantages, including improving the estimation of travel-times, providing higher number of early reflections for the tomography reconstruction, as well as a better space utilization. The accuracy of the reconstructed temperatures reveals that ATOM can meet the requirements of the indoor climate projects perfectly when it comes to the room air temperature distribution.

Acknowledgment

This study was funded by the Deutsche Forschungsgemeinschaft (DFG) under project number 465591632. Additionally, we highly appreciate the scientific collaboration with our project partners at the Chair of Acoustics and Haptics at the Technical University Dresden, and the Institute of Meteorology at the University of Leipzig.

References

Bleisteiner M, Barth M, Raabe A. 2016. Tomographic reconstruction of indoor spatial temperature distributions using room impulse responses. Measurement Science and Technology,27(3):35306.

Dokhanchi NS, Arnold J, Vogel A, Voelker C. 2019. Acoustic Travel-Time Tomography: Optimal Positioning of Transceiver and Maximal Sound-Ray Coverage of the Room. DAGA, 23–6.

Dokhanchi NS, Arnold J, Vogel A, Voelker C. 2020a. Measurement of indoor air temperature distribution using acoustic travel-time tomography: Optimization of transducers location and sound-ray coverage of the room. Measurement, 164:107934, https://doi.org10.1016/j.measurement.2020.107934.

Dokhanchi NS, Arnold J, Vogel A, Voelker C. 2020b. Reconstruction of the indoor air temperature distribution using acoustic travel-time tomography. Roomvent.

Fischer G, Barth M, Ziemann A. 2012. Acoustic tomography of the atmosphere: Comparison of different reconstruction algorithms. Acta Acustica united with Acustica, 98(4):534–45.

Franz S, Imbery C, Müller M, Bitzer J. 2015. Bestimmung des frequenzabhängigen akustischen Zentrums eines Lautsprechers im Zeitbereich. DAGA.

Srinivasan K, Sundararajan T, Narayanan S, Jothi TJS, Sarma CR. 2013. Acoustic pyrometry in flames. Measurement, 46(1):315–23.

Vorländer M. 2008. Auralization, Springer.

Ziemann A, Arnold K, Raabe A. 2002. Acoustic tomography as a remote sensing method to investigate the near-surface atmospheric boundary layer in comparison with in situ measurements. Journal of Atmospheric and Oceanic Technology, 19(8):1208–15.